

Entangling Two Individual Atoms of Different Isotopes via Rydberg Blockade

Yong Zeng,^{1,2,3} Peng Xu,^{1,2,*} Xiaodong He,^{1,2} Yangyang Liu,^{1,2,3} Min Liu,^{1,2} Jin Wang,^{1,2}
D. J. Papoular,⁴ G. V. Shlyapnikov,^{5,6,7,8} and Mingsheng Zhan^{1,2,†}

¹State Key Laboratory of Magnetic Resonance and Atomic and Molecular Physics,
Wuhan Institute of Physics and Mathematics,

Chinese Academy of Sciences—Wuhan National Laboratory for Optoelectronics, Wuhan 430071, China

²Center for Cold Atom Physics, Chinese Academy of Sciences, Wuhan 430071, China

³School of Physical Sciences, University of Chinese Academy of Sciences, Beijing 100049, China

⁴LPTM, UMR8089 of CNRS and Université de Cergy-Pontoise, F-95302 Cergy-Pontoise, France

⁵LPTMS, UMR8626 of CNRS and Université Paris-Sud, F-91405 Orsay, France

⁶SPEC, CEA & CNRS, Université Paris-Saclay, CEA Saclay, F-91191 Gif-sur-Yvette, France

⁷Russian Quantum Center, Novaya Street, Skolkovo, Moscow Region R-143025, Russia

⁸Van der Waals-Zeeman Institute, Institute of Physics, University of Amsterdam, The Netherlands

(Received 12 March 2017; published 18 October 2017)

We report on the first experimental realization of the controlled-NOT (CNOT) quantum gate and entanglement for two individual atoms of different isotopes and demonstrate a negligible cross talk between two atom qubits. The experiment is based on a strong Rydberg blockade for ^{87}Rb and ^{85}Rb atoms confined in two single-atom optical traps separated by $3.8\ \mu\text{m}$. The raw fidelities of the CNOT gate and entanglement are 0.73 ± 0.01 and 0.59 ± 0.03 , respectively, without any corrections for atom loss or trace loss. Our work has applications for simulations of many-body systems with multispecies interactions, for quantum computing, and for quantum metrology.

DOI: 10.1103/PhysRevLett.119.160502

Quantum entanglement is crucial for simulating and understanding exotic physics of strongly correlated many-body systems [1–3] and it is the key quantity for quantum information processing [4–6]. Entanglement of nonidentical particles provides a richer correlation physics, and for quantum information the interspecies entanglement has unique advantages in connecting quantum networks [7] for quantum nondemolition readout and for memory protection [8,9]. The entanglement of different qubits [10] has recently been demonstrated for two different ions [11,12].

Among various platforms that have allowed the realization of quantum entanglement, trapped neutral atoms offer unique possibilities for quantum computing and simulations. This is because, in contrast to ions, they allow for an excellent control of the interaction strength over 12 orders of magnitude [5,13] and for the creation of tunable multidimensional arrays of single atoms [14]. Although important experiments have been done towards realizing useful quantum information processing and quantum simulation with atomic systems [14–20], there are several primary challenges to be solved [10]. One of them is quantum nondemolition (QND) and low cross talk qubit measurement with a few μm qubit spacing. The two-element neutral atom system shows an important advantage here, since substantially different resonant frequencies of the two species allow the spectral isolation and individual addressing of the qubits. Also, manipulating multielement single atoms can provide extra degrees of freedom for quantum simulations. In realizing a Rydberg quantum

simulator [21] another species atomic qubit can work as an auxiliary qubit to manipulate or mediate the many-body spin interaction in target qubits, or provide a dissipative element when being optically pumped.

In this Letter, we present the first realization of quantum entanglement of two individual neutral atoms of different isotopes. We obtain an entangled state of ^{87}Rb and ^{85}Rb atoms confined in single-atom optical traps separated by $3.8\ \mu\text{m}$. The entanglement is generated from a heteronuclear CNOT quantum gate, which is created using the Rydberg blockade. We encode the control qubit in the ground hyperfine states $|F=1, M_F=0\rangle = |\downarrow\rangle$ and $|2, 0\rangle = |\uparrow\rangle$ of ^{87}Rb , whereas the target qubit is encoded in the states $|2, 0\rangle = |\downarrow\rangle$ and $|3, 0\rangle = |\uparrow\rangle$ of ^{85}Rb . For both atoms, the Rydberg state is $|r\rangle = |79D_{5/2}, m_j = 5/2\rangle$. Unlike in the case of the same atoms, we exploit the difference in the resonant frequencies of the two atoms to individually address and manipulate them. In this way, we ensure a negligible cross talk during state measurements and qubit operations at short interatomic separations. This makes the entanglement of different isotopes very different from the entanglement of identical atoms that are distinguishable by their spatial location with no overlap of their wave functions like in the experiment of Ref. [22].

The experimental apparatus and the single-atom trapping procedure for ^{87}Rb and ^{85}Rb atoms have been described in our recent work [23] [see Fig. 1(b)]. We then optically pump ^{87}Rb to the $|\uparrow\rangle$ state and ^{85}Rb to the $|\uparrow\rangle$ state. After

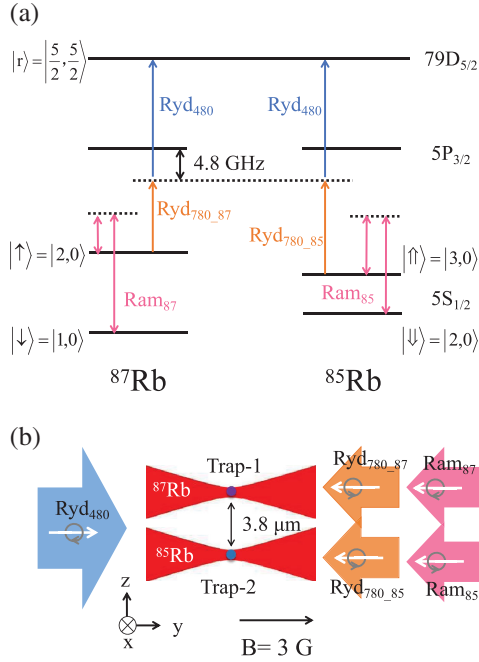


FIG. 1. Experimental setup. (a) Energy levels and lasers for ^{87}Rb and ^{85}Rb . Atoms are excited to Rydberg states through Raman transitions using 480 (Ryd_{480}) and 780 nm (Ryd_{780}) σ^+ -polarized lasers. The laser Ryd_{480} is blue detuned by 4.8 GHz from the intermediate state, and its waist $12.8 \mu\text{m}$ covers both atoms. The lasers Ryd_{780-87} and Ryd_{780-85} , whose frequencies differ by 1.13 GHz, address ^{87}Rb and ^{85}Rb . The degeneracy of the Rydberg states $|79D_{5/2}, m_j\rangle$ is lifted by the static magnetic field $B = 3 \text{ G}$ along the quantization axis y , and the laser frequencies are resonant with the $m_j = 5/2$ state. Single qubit operations are performed through Raman transitions using the 795 nm lasers Ram_{85} and Ram_{87} , which are red detuned by 50 GHz from the $5S_{1/2} \rightarrow 5P_{1/2}$ transition. (b) Experimental geometry. Two 830 nm lasers have the beam waist $2.1 \mu\text{m}$ to form two dipole traps separated by $3.8 \mu\text{m}$ along the z direction.

that the trapping potentials are adiabatically lowered from 0.6 to 0.1 mK. Both microtraps have trapping frequencies $\omega_y/2\pi = 1.39 \pm 0.01 \text{ kHz}$ in the longitudinal direction and $\omega_r/2\pi = 16.9 \pm 0.1 \text{ kHz}$ in the radial direction [see Fig. 1(b)]. We measure the atom temperatures $T_{87} = 8 \pm 1$ and $T_{85} = 9 \pm 1 \mu\text{K}$ using the release and recapture method [24]. Next, we combine Rydberg excitation pulses and single qubit operations with Raman lasers in order to demonstrate the heteronuclear Rydberg blockade, implement the CNOT gate, and entangle the two heteronuclear atoms. It is worth noting that both dipole traps are turned off during $6 \mu\text{s}$ for adding the Rydberg excitation pulses. The atom loss induced by turning off the traps is less than 2% in our setup. At the end of each sequence, we detect the qubit state by using a resonant laser to “blow away” $|\uparrow\rangle$ and $|\uparrow\rangle$ atoms, so that the survival probabilities refer to the atoms in the $|\downarrow\rangle$ and $|\downarrow\rangle$ states.

As the first step of our experiment, we show a negligible cross talk between the two atom qubits in state

measurements and qubit operations. This is crucial for our setup because all lasers cover both atoms, and the individual addressing of a single atom relies on the frequency difference of ^{87}Rb and ^{85}Rb rather than on the spatial distribution. During qubit state measurements the resonant blow away laser of ^{85}Rb may destroy the coherent state of ^{87}Rb due to unwanted scattering since the laser is detuned 1.1 GHz from ^{87}Rb , and vice versa. We check this influence by adding the blow away pulse of ^{85}Rb in between the ^{87}Rb ground state Rabi oscillation and the ^{87}Rb blow away pulse. We then compare the Rabi oscillations of ^{87}Rb with and without the pulse of ^{85}Rb as shown in Fig. 2(a). The amplitudes of the Rabi oscillations are equal within the measurement uncertainty, which shows a negligible cross talk in the state measurement. For Rydberg excitation, we use the two-photon transitions with the total Rabi frequency of about 1 MHz as shown in Fig. 1. Thus, the GHz spectral difference can provide enough protection for the qubit operations with each single atom. We also observe almost no excitation of ^{85}Rb when adding the Rydberg excitation laser of ^{87}Rb as shown in Fig. 2(b). Thanks to the negligible cross talk between the two atom qubits, we can put two atoms close enough to each other to reach a sufficiently strong Rydberg interaction for suppressing the blockade errors.

To demonstrate the heteronuclear Rydberg blockade, we first calculate the expected Rydberg blockade shift, which is different from that for the same atoms. If both atoms are in the $|r\rangle$ state, their interaction is dominated by the Förster resonance between the two-atom states in the $(79d_{5/2}, 79d_{5/2})$, $(80p_{3/2}, 78f)$, and $(81p_{3/2}, 77f)$ manifolds. We restrict the Förster interaction Hamiltonian to a subspace spanned by 436 states corresponding to distinguishable

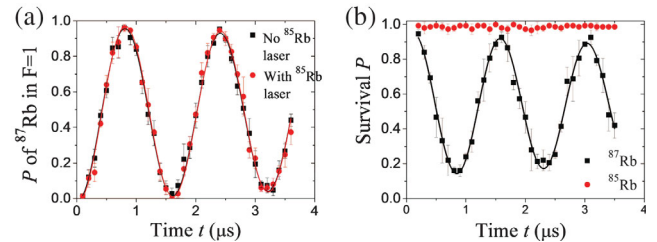


FIG. 2. Cross talk between ^{85}Rb and ^{87}Rb . (a) Rabi oscillations between the ^{87}Rb $|\uparrow\rangle$ and $|\downarrow\rangle$ states of ^{87}Rb (black squares). The red circles show the experimental data obtained when using the ^{85}Rb blow away laser before measuring the state of ^{87}Rb . The solid curves are damped sinusoidal fits $P = P_0 + Ae^{-t/t_0} \cos[2\pi f(t - t_c)]$, with $A = 0.49 \pm 0.01$, $f = 0.625 \pm 0.002 \text{ MHz}$, and $t_0 = 28 \pm 7 \mu\text{s}$ for black squares and $A = 0.50 \pm 0.02$, $f = 0.625 \pm 0.003 \text{ MHz}$, $t_0 = 27 \pm 15 \mu\text{s}$ for red circles. (b) The ^{87}Rb Rydberg excitation laser covers both ^{87}Rb in trap 1 (black squares) and ^{85}Rb in trap 2 (red circles). The ^{87}Rb atom shows coherent Rabi oscillations between the $|\uparrow\rangle$ and $|r\rangle$ states. The solid curves are damped sinusoidal fits with $A = 0.41 \pm 0.01$, $f = 0.685 \pm 0.008 \text{ MHz}$, and $t_0 = 19 \pm 5 \mu\text{s}$. The ^{85}Rb atom is almost unaffected, which shows a negligible cross talk.

atoms. Taking the initial two-atom state $|r\uparrow\rangle$ we account for its coupling to the Förster states and calculate the time evolution of the probability for both atoms to be in any of the excited Rydberg states taking part in the Förster resonance, $P_{85}(y, t) = 1 - |\langle r\uparrow | e^{-iHt/\hbar} | r\uparrow \rangle|^2$, and its average over time, $P_{85}(y)$. The latter depends on the offset $y = |y_2 - y_1|$ of the two atoms along the y direction. The blockade shift $\Delta E(y)$ is deduced from the relation $P_{85}(y) = (\hbar\Omega_{85})^2 / [(\hbar\Omega_{85})^2 + \Delta E^2]$ [25], where Ω_{85} is the effective Rabi frequency for ^{85}Rb . At zero temperature, for the distance $z = 3.8 \mu\text{m}$ between the microtraps, assuming a spatial offset $y = 1 \mu\text{m}$, the effective Rydberg interaction between the atoms is close to the strongly interacting Förster regime [5]. Accordingly, the numerical results yield $P_{85} \approx 10^{-6}$ and a very large blockade shift $\Delta E/h = 600 \text{ MHz}$ [26]. The finite temperature of the atoms causes them to explore larger values of the offset, $y \gtrsim 10 \mu\text{m}$, leading to the mean double-excitation probability $\langle P_{85} \rangle \approx 0.013$ for our temperatures $T_{87} = 8$ and $T_{85} = 9 \mu\text{K}$.

We realize the Rydberg blockade by applying a Rydberg π pulse on ^{87}Rb , waiting for $0.3 \mu\text{s}$, and applying a Rydberg pulse of variable duration on ^{85}Rb [Fig. 3(a)]. We measure the Rabi oscillations between the ^{85}Rb $|\uparrow\rangle$ and $|r\rangle$ states as a function of the second pulse duration [Fig. 3(b)]. The Rydberg states are detected through the atom loss with an efficiency of $\sim 90\%$, and the Rydberg excitation efficiency for ^{87}Rb and ^{85}Rb is $\sim 96\%$ (see Supplemental Material [26]). The lifetime of the $|r\rangle$ state is over $180 \mu\text{s}$, providing a long enough blockade for ^{85}Rb . We do not record the experimental data when ^{87}Rb is still in the trap after the sequence, so as to eliminate unblocked events when ^{87}Rb is not excited to the $|r\rangle$ state. The peak-to-peak amplitude of ^{85}Rb Rabi oscillations between the $|\uparrow\rangle$ and $|r\rangle$ states is 0.91 ± 0.02 in the absence of ^{87}Rb in trap 1 [Fig. 3(b)]. In

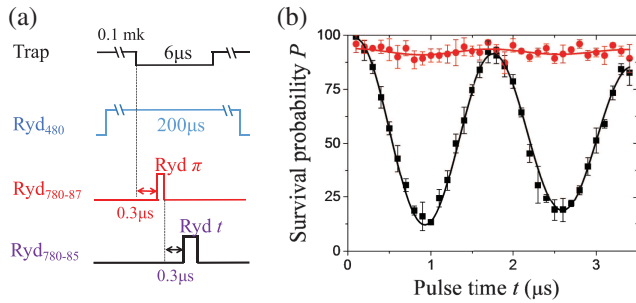


FIG. 3. Heteronuclear Rydberg blockade. (a) Time sequence. (b) Rabi oscillations between the ^{85}Rb $|\uparrow\rangle$ and $|r\rangle$ states. The experimental data are shown both in the absence (black squares) and in the presence (red circles) of ^{87}Rb in trap 1. The solid curves are damped sinusoidal fittings with $P = P_0 + Ae^{-t/t_0} \cos[2\pi f(t - t_c)]$. The fitting parameters are $A = 0.455 \pm 0.008$, $f = 0.600 \pm 0.003 \text{ MHz}$, $t_0 = 10 \pm 1 \mu\text{s}$ for black squares. We preset $f = 0.6 \text{ MHz}$, $t_0 = 10 \mu\text{s}$ for red circles to get $A = 0.017 \pm 0.006$. Each data point is an average value of 150 measurements.

its presence, the experimental data show a strong Rydberg blockade that suppresses the oscillation amplitude to 0.03 ± 0.01 , in accordance with our theoretical prediction. The remaining weak oscillations of ^{85}Rb are mainly due to not perfect experimental conditions, including the loss of ^{87}Rb and transitions to other Rydberg states.

Next, we use the Rydberg blockade to generate a heteronuclear CNOT gate following the protocol of Ref. [32]. This involves three Rydberg pulses [Fig. 4(a)]: (i) a π pulse on ^{87}Rb between the $|\uparrow\rangle$ and $|r\rangle$ states, (ii) a 2π pulse on ^{85}Rb between $|\uparrow\rangle$ and $|r\rangle$, and (iii) a π pulse on ^{87}Rb between $|r\rangle$ and $|\uparrow\rangle$. Then, combining two Hadamard gates realized using Raman $\pi/2$ pulses between the $|\uparrow\rangle$ and $|\downarrow\rangle$ states, we demonstrate the heteronuclear CNOT gate shown in Fig. 4. Its intrinsic coherence is illustrated by measuring the oscillation of the output probabilities as a function of the relative phase between the two Hadamard gates [Fig. 4(b)]. Setting the relative phase to 0 (π), the CNOT gate will flip the target qubit if the control qubit is $|\uparrow\rangle$ ($|\downarrow\rangle$).

The fidelity of the CNOT gate is determined by measuring its truth table probabilities [Fig. 4(c)]. We add an extra Raman π pulse before acting with the blow away laser to transfer the $|\uparrow\rangle$ state ^{87}Rb atoms to $|\downarrow\rangle$ and the $|\uparrow\rangle$ state ^{85}Rb atoms to $|\downarrow\rangle$, in order to exclude other atom losses as in Ref. [33]. The raw fidelity of the CNOT gate is $F = \text{Tr}[|U_{\text{ideal}}^T|U_{\text{CNOT}}|]/4 = 0.73(1)$. It is mainly limited by technical reasons and can be improved by stabilizing the Raman pulse powers and by increasing the Rydberg excitation efficiency.

Finally, we generate a heteronuclear entangled state of ^{87}Rb and ^{85}Rb . Starting with the two-atom state

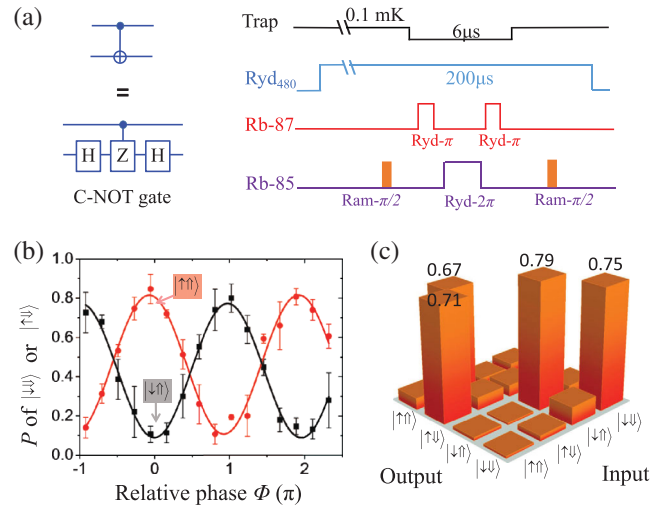


FIG. 4. Heteronuclear CNOT gate. (a) Experimental time sequence. (b) Output states as a function of the relative phase between the Raman $\pi/2$ pulses, for the initial states $|\downarrow\uparrow\rangle$ (black squares) and $|\uparrow\uparrow\rangle$ (red circles). The solid curves are sinusoidal fits yielding the phase difference of $(0.94 \pm 0.01)\pi$ between the two signals. (c) Measured truth table matrix U_{CNOT} for the CNOT gate with the relative phase between the $\pi/2$ pulses set to 0 .

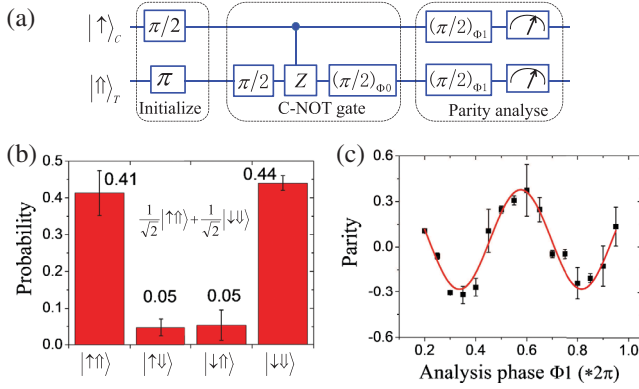


FIG. 5. Entanglement of two heteronuclear atoms. (a) Time sequence. (b) Measured probabilities for the entangled state. (c) The parity signal P . The solid curve is a sinusoidal fit with $P = 2\text{Re}(C_2) - 2|C_1|\cos(2\phi_1 + \xi)$, where $\text{Re}(C_2) = 0.02 \pm 0.02$, $|C_1| = 0.16 \pm 0.01$.

$(|\uparrow\rangle + i|\downarrow\rangle)|\downarrow\rangle/\sqrt{2}$, we apply the CNOT gate to create the entangled state $(|\uparrow\uparrow\rangle + |\downarrow\downarrow\rangle)/\sqrt{2}$. In order to quantify the entanglement of our created Bell state, we measure the coherence C_1 between the $|\uparrow\uparrow\rangle$ and $|\downarrow\downarrow\rangle$ states by studying the response of the system to the simultaneous rotation of the two qubits [34]. For that purpose, we apply to both atoms $\pi/2$ pulses carrying the same phase ϕ_1 relative to the initial pulses [Fig. 5(a)] and measure the oscillations of the parity signal $P = P_{\uparrow\uparrow} + P_{\downarrow\downarrow} - P_{\uparrow\downarrow} - P_{\downarrow\uparrow}$ as a function of ϕ_1 [Fig. 5(c)]. This gives us access [30,34] to the coherence $|C_1| = 0.16 \pm 0.01$ which, combined with the populations $P_{\uparrow\uparrow} = 0.41$ and $P_{\downarrow\downarrow} = 0.44$ [Fig. 5(b)], leads to the entangled state fidelity $F = (P_{\uparrow\uparrow} + P_{\downarrow\downarrow})/2 + |C_1| = 0.59 \pm 0.03$. The obtained fidelity is clearly above the threshold of 0.5 ensuring the presence of entanglement. We obtain it without any corrections for atom or trace losses. It is lower than the fidelity of our CNOT gate mainly because of the motion of ^{87}Rb . Following Ref. [30] we evaluate that at our temperatures and CNOT gate fidelity the upper bound of the entanglement fidelity is $F_{\text{ent-max}} = 0.65$, which is somewhat above our experimental result.

To conclude, we have realized a CNOT gate between two individual single atoms of different isotopes and demonstrated a negligible cross talk between two atom qubits. The gate is based on a strong heteronuclear Rydberg blockade, and the raw fidelity is 0.73 ± 0.01 . The entanglement of two different atoms is then deterministically generated with the raw fidelity 0.59 ± 0.03 . Our work makes a significant step towards the manipulation of heteronuclear atom systems. We use a difference in the transition frequencies to individually address a single atom. Therefore, two atoms can be put at a short separation while maintaining individual addressing to explore the physics in a very strong Rydberg interaction regime [35]. Moreover, the atoms of

different species can be trapped in an array with an arbitrary geometry to realize a Rydberg quantum simulator of exotic spin models, such as the Kitaev toric code, color code, or coherent energy transfer [21]. The difficulty for one to create a pattern with dozens of single atoms of different species is no more than those works done recently with the same species atoms [19,20]. That is, single atoms are first loaded into a large ensemble of dipole traps randomly, and then a deeper moveable trap is used to transport single atoms into different traps of desired pattern. Our results pave a way towards quantum computing with heteronuclear systems [10] and towards the realization of high fidelity state detection, which has recently been predicted not to have any fundamental limit even at room temperature [31].

This work was supported by the National Key Research and Development Program of China under Grants No. 2016YFA0302800, No. 2017YFA0304501, and No. 2016YFA0302002, the Strategic Priority Research Program of the Chinese Academy of Sciences under Grant No. XDB21010100, the National Natural Science Foundation of China under Grants No. 11674361 and No. 11227803, and Youth Innovation Promotion Association CAS No. 2017378. D.J.P. and G.V.S. acknowledge support from IFRAF and emphasize that the research leading to their results in this Letter has received funding from the European Research Council under the European Community's Seventh Framework Programme (FP7/2007-2013 Grant Agreement No. 341197).

*etherxp@wipm.ac.cn

†mszhan@wipm.ac.cn

- [1] S. Sachdev, Emergent gauge fields and the high-temperature superconductors, *Phil. Trans. R. Soc. A* **374**, 20150248 (2016).
- [2] N. Laflorencie, Quantum entanglement in condensed matter systems, *Phys. Rep.* **646**, 1 (2016).
- [3] L. Amico, R. Fazio, A. Osterloh, and V. Vedral, Entanglement in many-body systems, *Rev. Mod. Phys.* **80**, 517 (2008).
- [4] M. A. Nielsen and I. L. Chuang, *Quantum Computation and Quantum Information* (Cambridge University Press, Cambridge, England, 2000).
- [5] M. Saffman, T.G. Walker, and K. Mølmer, Quantum information with Rydberg atoms, *Rev. Mod. Phys.* **82**, 2313 (2010).
- [6] D. Leibfried, M.D. Barrett, T. Schaetz, J. Britton, J. Chiaverini, W.M. Itano, J.D. Jost, C. Langer, and D.J. Wineland, Toward Heisenberg-limited spectroscopy with multiparticle entangled states, *Science* **304**, 1476 (2004).
- [7] B. B. Blinov, D. L. Moehring, L. M. Duan, and C. Monroe, Observation of entanglement between a single trapped atom and a single photon, *Nature (London)* **428**, 153 (2004).
- [8] M. Schulte, N. Lorch, I. D. Leroux, P. O. Schmidt, and K. Hammerer, Quantum Algorithmic Readout in Multi-Ion Clocks, *Phys. Rev. Lett.* **116**, 013002 (2016).

- [9] I. I. Beterov and M. Saffman, Rydberg blockade, Forster resonances, and quantum state measurements with different atomic species, *Phys. Rev. A* **92**, 042710 (2015).
- [10] M. Saffman, Quantum computing with atomic qubits and Rydberg interactions: progress and challenges, *J. Phys. B* **49**, 202001 (2016).
- [11] C. J. Ballance, V. M. Schafer, J. P. Home, D. J. Szwer, S. C. Webster, D. T. C. Allcock, N. M. Linke, T. P. Harty, D. P. L. A. Craik, D. N. Stacey, A. M. Steane, and D. M. Lucas, Hybrid quantum logic and a test of Bell's inequality using two different atomic isotopes, *Nature (London)* **528**, 384 (2015).
- [12] T. R. Tan, J. P. Gaebler, Y. Lin, Y. Wan, R. Bowler, D. Leibfried, and D. J. Wineland, Multi-element logic gates for trapped-ion qubits, *Nature (London)* **528**, 380 (2015).
- [13] C. Chin, R. Grimm, P. Julienne, and E. Tiesinga, Feshbach resonances in ultracold gases, *Rev. Mod. Phys.* **82**, 1225 (2010).
- [14] H. Labuhn, D. Barredo, S. Ravets, S. de Leseleuc, T. Macri, T. Lahaye, and A. Browaeys, Tunable two-dimensional arrays of single Rydberg atoms for realizing quantum Ising models, *Nature (London)* **534**, 667 (2016).
- [15] A. M. Kaufman, B. J. Lester, M. Foss-Feig, M. L. Wall, A. M. Rey, and C. A. Regal, Entangling two transportable neutral atoms via local spin exchange, *Nature (London)* **527**, 208 (2015).
- [16] Y. Y. Jau, A. M. Hankin, T. Keating, T. H. Deutsch, and G. W. Biedermann, Entangling atomic spins with a Rydberg-dressed spin-flip blockade, *Nat. Phys.* **12**, 71 (2016).
- [17] T. Xia, M. Lichtman, K. Maller, A. W. Carr, M. J. Piotrowicz, L. Isenhower, and M. Saffman, Randomized Benchmarking of Single-Qubit Gates in a 2D Array of Neutral-Atom Qubits, *Phys. Rev. Lett.* **114**, 100503 (2015).
- [18] Y. Wang, A. Kumar, T. Y. Wu, and D. S. Weiss, Single-qubit gates based on targeted phase shifts in a 3D neutral atom array, *Science* **352**, 1562 (2016).
- [19] D. Barredo, S. de Leseleuc, V. Lienhard, T. Lahaye, and A. Browaeys, An atom-by-atom assembler of defect-free arbitrary two-dimensional atomic arrays, *Science* **354**, 1021 (2016).
- [20] M. Endres, H. Bernien, A. Keesling, H. Levine, E. R. Anschuetz, A. Krajenbrink, C. Senko, V. Vuletic, M. Greiner, and M. D. Lukin, Cold Matter Assembled Atom-by-Atom, *Science* **354**, 1024 (2016).
- [21] H. Weimer, M. Muller, I. Lesanovsky, P. Zoller, and H. P. Buchler, A Rydberg quantum simulator, *Nat. Phys.* **6**, 382 (2010).
- [22] H. Krauter, C. A. Muschik, K. Jensen, W. Wasilewski, J. M. Petersen, J. I. Cirac, and E. S. Polzik, Entanglement generated by dissipation and steady state entanglement of two macroscopic objects, *Phys. Rev. Lett.* **107**, 080503 (2011).
- [23] P. Xu, J. H. Yang, M. Liu, X. D. He, Y. Zeng, K. P. Wang, J. Wang, D. J. Papoular, G. V. Shlyapnikov, and M. S. Zhan, Interaction-induced decay of a heteronuclear two-atom system, *Nat. Commun.* **6**, 7803 (2015).
- [24] C. Turchander, A. M. Lance, A. Browaeys, Y. R. P. Sortais, and P. Grangier, Energy distribution and cooling of a single atom in an optical tweezer, *Phys. Rev. A* **78**, 033425 (2008).
- [25] E. Urban, T. A. Johnson, T. Henage, L. Isenhower, D. D. Yavuz, T. G. Walker, and M. Saffman, Observation of Rydberg blockade between two atoms, *Nat. Phys.* **5**, 110 (2009).
- [26] See Supplemental Material at <http://link.aps.org/supplemental/10.1103/PhysRevLett.119.160502> for details of laser system, error budget of entanglement, and calculations of heteronuclear Rydberg blockade, which includes Refs. [5, 25, 27–31].
- [27] A. Browaeys, D. Barredo, and T. Lahaye, Experimental investigations of dipole-dipole interactions between a few Rydberg atoms, *J. Phys. B* **49**, 152001 (2016).
- [28] K. M. Maller, M. T. Lichtman, T. Xia, Y. Sun, M. J. Piotrowicz, A. W. Carr, L. Isenhower, and M. Saffman, Rydberg-blockade controlled-not gate and entanglement in a two-dimensional array of neutral-atom qubits, *Phys. Rev. A* **92**, 022336 (2015).
- [29] A. Gaetan, Y. Miroshnychenko, T. Wilk, A. Chotia, M. Viteau, D. Comparat, P. Pillet, A. Browaeys, and P. Grangier, Observation of collective excitation of two individual atoms in the Rydberg blockade regime, *Nat. Phys.* **5**, 115 (2009).
- [30] T. Wilk, A. Gaetan, C. Evellin, J. Wolters, Y. Miroshnychenko, P. Grangier, and A. Browaeys, Entanglement of Two Individual Neutral Atoms Using Rydberg Blockade, *Phys. Rev. Lett.* **104**, 010502 (2010).
- [31] L. S. Theis, F. Motzoi, F. K. Wilhelm, and M. Saffman, High-fidelity Rydberg-blockade entangling gate using shaped, analytic pulses, *Phys. Rev. A* **94**, 032306 (2016).
- [32] D. Jaksch, J. I. Cirac, P. Zoller, S. L. Rolston, R. Cote, and M. D. Lukin, Fast Quantum Gates for Neutral Atoms, *Phys. Rev. Lett.* **85**, 2208 (2000).
- [33] L. Isenhower, E. Urban, X. L. Zhang, A. T. Gill, T. Henage, T. A. Johnson, T. G. Walker, and M. Saffman, Demonstration of a Neutral Atom Controlled-NOT Quantum Gate, *Phys. Rev. Lett.* **104**, 010503 (2010).
- [34] Q. A. Turchette, C. S. Wood, B. E. King, C. J. Myatt, D. Leibfried, W. M. Itano, C. Monroe, and D. J. Wineland, Deterministic Entanglement of Two Trapped Ions, *Phys. Rev. Lett.* **81**, 3631 (1998).
- [35] Compared to the 2 atoms of different elements, the hyperfine structure splitting of distinct isotopes of the same element is in the above GHz level, and the splitting of Rydberg energy levels is small. As we demonstrate in experiments, in two-photon Rydberg excitation, 2 isotope atoms can conveniently use a single 480 nm laser beam. This greatly simplifies the experimental system of lasers. In addition, the ac-Stark frequency shift of the different atoms of the same element is small and the same dipole trap laser system can be used. The challenge with distinct isotopes lies on the GHz laser wavelength difference, which is much smaller than those used for distinct elements. The small difference may cause cross talk error. But our current experiment does not detect any cross talk error.